Journal of Non-Crystalline Solids 116 (1990) 27–32
North-Holland

XANES STUDY OF STRUCTURAL DISORDER IN AMORPHOUS SILICON

A. DI CICCO, A. BIANCONI, C. COLUZZA and P. RUDOLF
Dipartimento di Fisica, Università di Roma "La Sapienza", 00185 Roma, Italy

P. LAGARDE and A.M. FLANK
LURE, CEA–CNRS–MEN, Université Paris Sud, Bat. 209D, Orsay, France

A. MARCELLI
Laboratori Nazionali di Frascati, INFN, 00044 Frascati, Italy

Received 31 October 1988
Revised manuscript received 22 September 1989

An investigation of the structure of several amorphous silicon (a-Si) films is presented. Samples were prepared by using the ion beam sputtering technique at different substrate deposition temperatures. X-ray absorption spectroscopy and multiple scattering formalism have been used to detect structural variations of the a-Si films. The analysis of the XANES (X-ray absorption near-edge structure) spectra shows that increasing the substrate deposition temperature leads to a structural change toward a higher-level short-range order.

1. Introduction

Hydrogenated amorphous silicon (a-Si : H) has recently attracted technological interest for application to devices. Moreover the correlation between growth parameters and optoelectronic properties is not yet well clarified. In order to separate the effect of the hydrogen from the deposition temperature effect [1,2] on the amorphous matrix disorder, we investigate several amorphous silicon (a-Si) films, prepared in different conditions, by means of X-ray absorption spectroscopy (XAS). Analysis on unhydrogenated a-Si samples is important also from the theoretical point of view because XAS can give information beyond the radial distribution function.

XAS is a structural technique which contains information about bond distance distribution via EXAFS (extended X-ray absorption fine structure) and disorder in bond angles via XANES (X-ray absorption near edge structure) analysis. Recent advances in data analysis of XAS have stimulated a great amount of work both from theoretical and from experimental points of view [3,4].

Many recent papers have pointed out that spherical wave formalism and multiple scattering effects are essential for the interpretation of the low-energy side of the absorption spectra. In particular, it has been shown that a multiple scattering signal can be extracted from an absorption spectrum by using the recently demonstrated expansion [5–7]:

$$\alpha(k) = \alpha_0(k)\left[1 + \sum_{n=2}^{\infty} \chi_n(k)\right].$$

The absorption spectrum is described through a sum of χ_n terms due to the scattering paths of the photoelectron involving $n-1$ atoms around the photoabsorber. Here χ_2 is the usual EXAFS term, due to the single scattering, which is dominant at high energies of the photoelectron and probes the pair correlation function. The χ_n terms can be important in the XANES part of the spectra and probe the higher-order correlation functions.

X-ray or neutron diffraction investigation on amorphous systems furnish only the one-dimensional correlation function and cannot discriminate between structures with different levels of short-range order (see for example ref. [9]). Therefore the analysis of XANES spectra can be unique technique for understanding structural properties of amorphous materials.

XANES and EXAFS analysis of crystal silicon [7,8] have shown that the χ_3 signal plays an important role. Disorder in bond angles in amorphous silicon produces a decrease in the intensity of the χ_3 contribution to the absorption spectrum.

The aim of this analysis is to investigate changes in the XANES experimental spectra in order to understand some characteristics of the ordering process obtained increasing the substrate deposition temperature.

2. Experimental

Thin a-Si films (~ 1.5 μm) have been prepared by ion-beam sputtering [10] employing a 500 eV Ar beam to sputter silicon from a polycrystal target to a heated beryllium substrate. The samples have been deposited at three different substrate deposition temperatures: room temperature, 200 °C and 400 °C. Films obtained with this method appear to be amorphous and homogeneous throughout as shown by standard X-ray diffraction analysis (see for example ref. [11]).

X-ray absorption measurements were recorded in transmission mode at the synchrotron radiation dedicated storage ring ACO (Orsay) by using a double InSb(111) crystal monochromator and one ionization chamber as photon detector.

3. Results and discussion

X-ray absorption spectra of different a-Si films (deposited at room temperature, 200 °C and 400 °C) are reported in fig. 1.

In the EXAFS energy range (for wave vector values $k > 4$ Å^{-1}, where $k = (1/\hbar)\sqrt{2m(E - E_0)}$ and $E_0 \approx 1836$ eV) there are no significant differences between the spectra. On the other hand the high-resolution XANES part of the spectra is very sensitive to the growth conditions, i.e. to the local ordering, of the samples. These differences concern the modulating part of the absorption coefficients and they can easily be observed by considering the first derivatives of the spectra (derivatives' box in fig. 1).

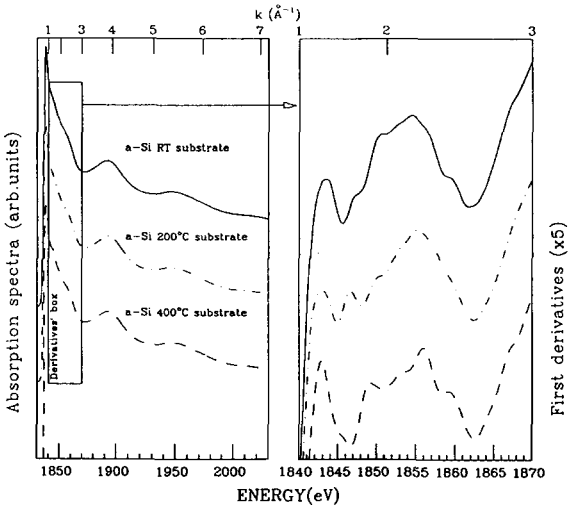

Fig. 1. X-ray absorption spectra of different amorphous silicon (a-Si) samples. The left panel contains the normalized absorption spectra of each sample described in the text, the right one the derivatives of each spectrum drawn in the XANES energy range where there are relevant differences between the spectra. In this energy range the accuracy is limited only from the noise on the experimental data that is, an average, less than 0.1%; the standard deviation is 0.0003.

The first step of the analysis is the evaluation of the modulating part of the absorption coefficient $\chi_{expt}(k)$, defined as:

$$\chi_{expt}(k) = [\alpha_K(k) - \alpha_0(k)]/\alpha_0(k),$$

where $\alpha_K(k)$ and $\alpha_0(k)$ are, respectively, the K-edge total absorption coefficient and the smooth atomic contribution. We have used a standard procedure [12] for removing $\alpha_0(k)$ from the experimental spectra. Particular care was taken for the choice of the absorption jump and of the energy threshold E_0 of each film spectrum in order to reduce amplitude and phase errors in the analysis.

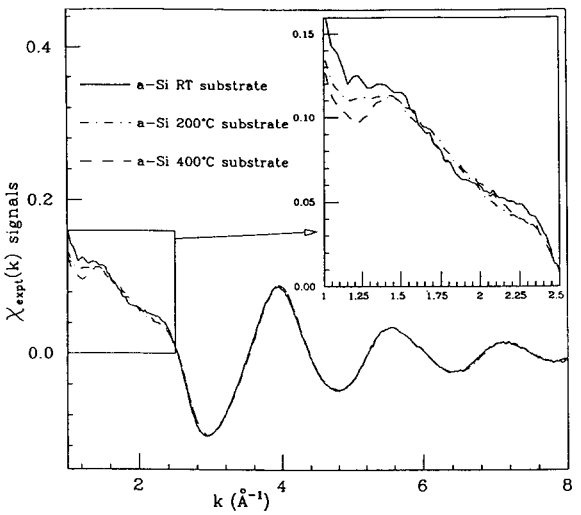

Fig. 2. $\chi_{expt}(k)$ signals of each a-Si sample. The low-energy part of the spectra has been enlarged in the panel inside the figure in order to show the different behaviour of the XANES spectra.

The $\chi_{expt}(k)$ signal contains information about local arrangement of the atoms around the photoabsorber which can be extracted by using the multiple scattering theory [3,9].

The $\chi_{expt}(k)$ signals relative to the three samples of a-Si are shown in fig. 2. In the EXAFS energy range we observe a regular oscillation due to the single scattering signal of the first neighbour coordination shell. We note also a characteristic peak of low intensity at about 5.8 Å^{-1}, always present in silicon K-edge absorption spectra and assigned to a double electron excitation [14].

A simple Fourier analysis shows that differences in XANES spectra cannot be assigned to a change in the first shell contribution but are due to higher frequency signals, identified as multiple scattering and single scattering second shell terms. This high frequency contribution is difficult to analyze quantitatively by Fourier-transform technique because the signal is too weak and energy-limited to give well-resolved peaks in the Fourier-transform spectrum. This approach gave good results in the case of amorphous germanium [15] where backscattering amplitudes are lower on the low-energy side of the spectra and a higher level of medium-range order was obtained increasing the substrate deposition temperature. Fourier-transform analysis was also used on a-Si [16] by considering only the peak positions.

In our case a subtraction procedure is more sensitive to variations of the high-frequency signals, moreover calculated multiple scattering contributions can be compared with the experimental spectra for obtaining structural information.

The multiple scattering expansion gives us a formula for analyzing XANES and EXAFS K-edge spectra [5–8]:

$$\alpha_K(k) = \alpha_0(k)\left[1 + \sum_{2\ n}^{\infty} \chi_n(k)\right], \tag{1}$$

$$\chi_{expt}(k) = \sum_{2\ n}^{\infty} \chi_n(k); \tag{2}$$

here $\chi_n(k)$ represents the contribution arising from all multiple scattering pathways p_n beginning and bending at the central atom and involving $n-1$ neighbouring atoms.

The general expression for $\chi_n(k)$ is given by

$$\chi_n(k) = \sum_{p_n} A_{p_n}(k)\ \sin\left[kR_{p_n} + \phi(k,\ p_n) + 2\delta_1^0\right]$$

$$= \sum_{p_n} A_{p_n}(k)\ \sin\left[\phi^{\text{eff}}(k,\ p_n)\right], \tag{3}$$

where R_{p_n} is the total length of the scattering path and δ_1^0 is the central atom phase shift. The amplitudes A_{p_n} decrease with increasing order n, so that usually $\chi_2(k)$ is the dominant term in the whole energy range.

Inelastic losses of the photoelectron in the final state, core hole lifetime and experimental resolution can be considered "a posteriori" for each particular path p_n by introducing an effective damping factor [8,17] $\exp(-R_{p_n}/\lambda_{\text{eff}})$ in the amplitudes.

A Debye–Waller-like damping factor $\exp[-2k^2\sigma_{p_2}^2]$ is required to take account of thermal disorder for crystalline materials in the single scattering contribution χ_2 due to the jth coordination shell. In amorphous systems it is sometimes necessary to consider the actual asymmetric pair distribution function.

For multiple scattering contributions χ_n, $n > 2$, the inclusion of the damping and phase effects due to thermal and static disorder is a problem

tackled very recently [18]. As a first approximation it is possible to consider again an effective Debye–Waller-like damping factor $\exp[-2k^2\sigma_{p_n}^2]$ for each particular path p_n.

Starting from these considerations we have used an effective total damping factor

$$\exp\left[-R_{p_n}/\lambda_{\text{eff}} - 2k^2\sigma_{p_n}^2\right] \tag{4}$$

for each multiple scattering path of interest in amorphous silicon.

In the remainder of the paper we take the sample deposited at room temperature (expected to have the most disordered structure) as a reference by considering the subtraction of its X-ray modulating signal from the other ones. Therefore, in terms of the multiple scattering expansion (2), we will consider a signal:

$$\begin{aligned} S_i(k) &= \chi_{\text{expt}}^{i}(k) - \chi_{\text{expt}}^{\text{RT}}(k) \\ &= \sum_{p_n} A_{p_n}(k)\,\sin\left[\phi^{\text{eff}}(k,\,p_n)\right] \\ &\quad \times \exp\left[-R_{p_n}/\lambda_{\text{eff}}\right]\left\{\left(Np_n^i\right)\exp\left[-2k^2\sigma_{p_n}^{i^2}\right]\right. \\ &\quad \left.-\left(Np_n^{\text{RT}}\right)\exp\left[-2k^2\sigma_{p_n}^{\text{RT}^2}\right]\right\}, \end{aligned} \tag{5}$$

where the index i runs over the X-ray absorption modulating signals of the a-Si samples prepared under different conditions.

By writing eq. (5) we assume that no dramatic structural changes occur in different a-Si samples in such a way that photoelectron paths of interest p_n, phase shifts, effective mean free path and average total length R_{p_n} are invariant. Mean square relative displacements (MSRDs) $\sigma_{p_n}^2$ (generalized to multiple scattering geometries) and effective coordination numbers Np_n of the paths are allowed to change from the XANES spectra of the room temperature sample to the others. These changes characterize the gradual transition to a more ordered phase.

Previous results on crystal [8] and amorphous [7,19] silicon K-edge spectra indicate that a small cluster which comprises only two shells of neighbour atoms can be sufficient to explain the amorphous silicon XANES spectra.

By considering such a 17-atom cluster inside the crystal silicon structure three major X-ray absorption signals can be found, apart from the main first shell signal of low frequency. In fig. 3 we show these relevant signals [7]: the single scattering χ_2 (2S2-type) contribution due to the second-shell atoms (upper curve); the double scattering χ_3 (3S2-type) signal due to the shortest triangular paths involving second-shell atoms (center curve); the χ_3 contribution (3S1-type) due to the shortest triangular paths inside the first-neighbour cluster (lower curve).

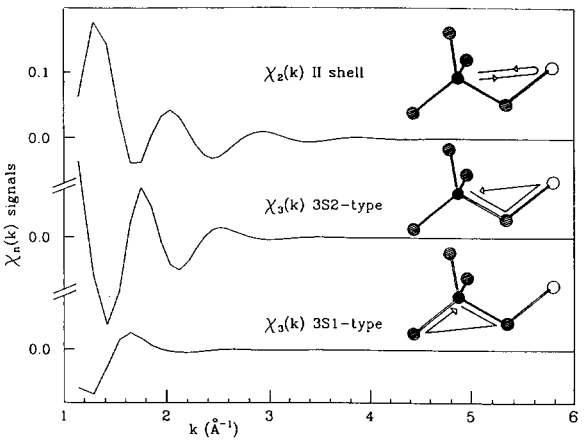

Fig. 3. Calculated χ_2 and χ_3 contributions to the Si K-edge absorption coefficient for the geometry of crystal silicon. On the right the scattering pathways of the photoelectron are drawn (the photoabsorbing atom is shown as a black sphere). The signals are strongly damped by using effective Debye–Waller-like factors $[\exp(-k^2\sigma_{p_n}^2)]$ expected for the amorphous silicon case.

A previous paper demonstrated how these signals are detectable in the case of crystal silicon [7]. In the transition from the amorphous to the crystalline phase an increase of these contributions has to be expected. Thus they can be adopted as signatures of ordering. In particular, a reduction of the MSRD of each p_n contribution can explain the differences in the XANES spectra of the different a-Si samples.

In fig. 3 the χ_2 and χ_3 signals are damped with reasonable values of MSRD which take into account both thermal and static disorder in amorphous silicon structure. These values were estimated starting from standard random-network models [20,21] and fitting procedures: $\sigma_{p_{2S2}}^2 = 0.09$ Å^2, $\sigma_{p_{3S1}}^2 = 0.08$ Å^2, $\sigma_{p_{3S2}}^2 = 0.10$ Å^2. The relevant

signals shown in fig. 3 cannot reproduce the actual high-frequency contribution in the RT-prepared a-Si because other higher-order multiple scattering signals are expected to be important (the χ_4 contribution inside the first shell, for example). However, these relevant χ_2 and χ_3 contribution can be used as a general guide in an investigation of the transition from the amorphous to the crystalline phase.

Analysis of the Fourier-filtered difference spectra (free from low-frequency contribution) can be carried out by taking advantage of eq. (5) and of the χ_2 and χ_3 calculated signals. We have assumed a maximum level of disorder, as it is justified by the preparation and the characterization of the samples, and fixed MSRD values in the room-temperature-prepared sample. In order to discuss the difference spectra we consider the three signals of fig. 3 which are dominant in the crystalline case by utilizing eq. (5) and limiting the series to the corresponding three paths.

A fitting procedure was employed, by using the MINUIT program of the CERN library, in order to compare experimental differences and theoretical signals.

In fig. 4 we compare experimental (solid curves) and calculated signals (dot-dashed curves). We have considered in the calculation the signals of fig. 3 (Fourier-filtered in the same range of the experimental differences) allowing the relative variation $\Delta\sigma_{p_n}^{i^2} = \sigma_{p_n}^{RT^2} - \sigma_{p_n}^{i^2}$ and Np_n^i parameters to change in order to obtain the best agreement with the experimental curve.

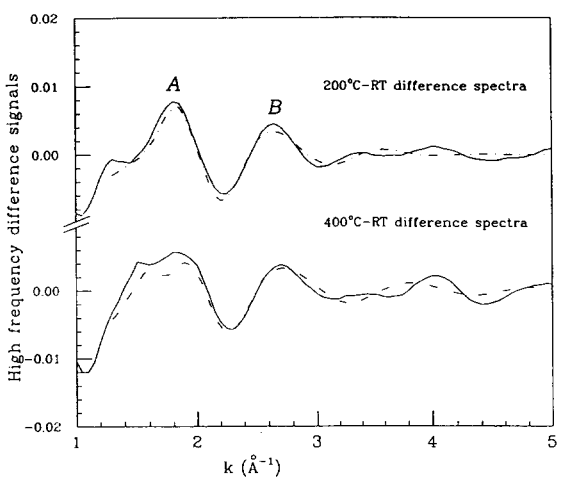

Fig. 4. XANES difference spectra of the $\chi_{expt}(k)$ signals of fig. 2. Solid curves are the experimental difference spectra filtered and free from low-frequency contributions. They are compared with calculated results (dot-dashed curves) obtained taking into account single and double scattering contributions.

Table 1
Parameter values obtained by best-fit calculation of the difference spectra of fig. 4. We report the calculated variation $\Delta\sigma_{p_n}^{i^2} = \sigma_{p_n}^{RT^2} - \sigma_{p_n}^{i^2}$ (where i indicates 200 °C and 400 °C-prepared a-Si samples) of the MSRDs relative to the three scattering paths p_n described in the text. Statistical errors are quoted in brackets. The ordering tendency obtained increasing the substrate deposition temperature of the a-Si sample is marked by the correspondent decrease of the MSRD values.

Path type p_n	$\Delta\sigma^2$ (200 °C)	$\Delta\sigma^2$ (400 °C)
3S1	0.04 (3)	0.06 (3)
3S2	0.022 (8)	0.030 (8)
2S2 (II shell)	0.004 (8)	0.027 (8)

Coordination number of each path in each sample were found to be the same within the experimental errors, while MSRDs showed changes which reflect the gradual ordering of the local structure. In table 1 the calculated variations of the MRSDs of each relevant path are reported. We quote also the statistical errors calculated using the standard procedures included in the MINUIT program: that is, we changed each fit parameter imposing the increase of the sum of the square deviations to be less than our confidence level, defined essentially by the noise in the experimental data (less than 0.1%).

Looking at table 1 and fig. 4 we recognize two steps in the gradual transition to the crystalline phase:

(1) *In the 200 °C-prepared sample a higher level of order is found inside the first-neighbour atoms coordination shell while second-shell atoms seem not to be involved in the ordering process.* In fact, we observe a remarkable change of the MSRDs relative to the 3S1-type path (completely inside the tetrahedron) and of the 3S2 one (which involves two atoms of the first shell) while the χ_2 second shell signal remains invariant. In fig. 4 this fact can be observed by noting that the main two peaks A and B of the experimental difference spectrum correspond to the convolution of the

analogous 3S1 and 3S2 peaks of the calculated signals of fig. 3.

(2) *In the 400 °C-prepared sample an increase in ordering of the second-shell atoms is found.* The important variation of the MSRD of the χ_2 second-shell signal indicates that the ordering process also involves the second-shell atoms. In fig. 4 the enlargement of the A peak, the slight shift of the B peak and the appearence of a feature at about 4 $Å^{-1}$ reflect the presence of a detectable second-shell signal in the 400 °C-prepared sample.

4. Conclusions

Investigation of X-ray absorption spectra of a-Si samples prepared in different conditions have shown structural differences. Spherical wave formalism and multiple scattering contributions have been used in the interpretation of the XANES difference spectra where the Fourier-transform method cannot give reliable results. Some features of the ordering process due to the increase of the substrate deposition temperature have been explained by comparison between calculated and experimental results.

The demonstrated sensitivity of the a-Si XANES spectra to the higher-order distribution function, i.e. to the bond and dihedral angle distributions, opens the way to the possibility of a direct comparison [22] with the realistic models of the atomic arrangement [23,24] which can be important in the determination of the structural properties of the amorphous systems.

References

[1] G.D. Cody, T. Tiedje, B. Abeles, B. Brooks and Y. Goldstein, Phys. Rev. Lett. 47 (1981) 1480.
[2] P. Rudolf, C. Coluzza, L. Mariucci and A. Frova, Phys. Scripta 37 (1988) 828.
[3] P. Lagarde, D. Raoux and J. Petiau, eds., Proc. Int. EXAFS and NES Conf., Fonteyraud (France), J. de Phys. 47, Coll. C8 (1986).
[4] R. Prinz and D. Koningsberger, eds 'X-ray Absorption: Principle, Applications, Techniques of EXAFS, SEXAFS, XANES" (Wiley, New York, 1987).
[5] C.R. Natoli and M. Benfatto, in ref. 3, p. 11.
[6] M. Benfatto, C.R. Natoli, A. Bianconi, J. Garcia, A. Marcelli, M. Fanfoni and I. Davoli, Phys. Rev. B34 (1986) 5774.
[7] A. Bianconi, A. Di Cicco, N.V. Pavel, M. Benfatto, A. Marcelli, C.R. Natoli, P. Pianetta and J. Woicik, Phys. Rev. B36 (1987) 6426.
[8] A. Di Cicco, N.V. Pavel and A. Bianconi, Sol. St. Commun. 61 (1987) 635.
[9] G. Etherington, A.C. Wright, J.T. Wenzel, J.C. Dore, J.H. Clarke and R.N. Sinclair, J. Non-Cryst. Solids 48 (1982) 265.
[10] S. Scaglione, C. Coluzza, D. Della Sala, L. Mariucci, A. Frova and G. Fortunato, Thin Solid Films 120 (1984) 215 and refs. therein.
[11] C. Coluzza, D. Della Sala, G. Fortunato, S. Scaglione and A. Frova, J. Non-Cryst. Solids 59 & 60 (1983) 723.
[12] B. Lengeler and P. Eisenberger, Phys.Rev. B21 (1980) 4507.
[13] P.A. Lee and J.B. Pendry, Phys. Rev. B11 (1975) 275.
[14] A. Filipponi, E. Bernieri and S. Mobilio, Phys. Rev. B38 (1988) 3298.
[15] F. Evangelisti, M.G. Proietti, A. Balzarotti, F. Comin. L. Incoccia and S. Mobilio. Sol. St. Commun. 37 (1981) 413.
[16] A. Menelle, A.M. Flank, P. Lagarde and R. Bellissent, ibid., ref. 3, p. 379.
[17] J.E. Muller, O. Jepsen and J.W. Wilkins, Sol. St. Commun. 42 (1982) 365.
[18] M. Benfatto, C.R. Natoli and A. Filipponi, Phys. Rev. B 40 (1989).
[19] A. Balerna, M. Benfatto, S. Mobilio, C.R. Natoli, A. Filipponi and F. Evangelisti, ibid., ref. 3, p. 63;
A. Di Cicco, A. Bianconi, C. Coluzza, P. Rudolf, P. Lagarde, A.M. Flank and A. Marcelli, Physica B158 (1989) 598.
[20] G.A.N. Connell and R.J. Temkin, Phys. Rev. B9 (1974) 5323.
[21] D.E. Polk and D.S. Bodreaux, Phys. Rev. Lett. 31 (1973) 92.
[22] A. Filipponi, A. Di Cicco, M. Benfatto and C.R. Natoli, in: Proc. 13th ICALS, Asheville, NC, 20–26 Aug. 1989, J. of Non-Cryst. Solids, to be published.
[23] F. Wooten, K. Winer and D. Weaire, Phys. Rev. Lett. 54 (1985) 1392.
[24] K. Winer, Phys. Rev. B35 (1987) 2366.